

Electronic Structure of $\text{Cr}(\text{NH}_3)_6^{3+}$ and Substituted Chromium(III) Ammine Compounds

L. G. Vanquickenborne,* B. Coussens, D. Postelmans, A. Ceulemans, and K. Pierloot

Received October 26, 1990

In this work, we present the first ab initio study for $\text{Cr}(\text{NH}_3)_6^{3+}$ and a number of mono- and disubstituted chromium(III) ammine compounds. This study concerns a detailed analysis of the ligand field spectra of the complexes. The ab initio results are discussed within the framework of a ligand field analysis of the different compounds and are compared with the available experimental data. The basic ligand field assumptions (additivity and transferability postulates) are confirmed. The theoretical ligand field parameters reflect the same relative donor properties of the ligands as the semiempirical ones. Yet—as a partial amendment of the ligand field picture—the result of a population analysis reveals that the ligand to metal donations show rather significant variations from one complex to another. In comparison with experiment, the quartet–quartet transitions are reasonably well predicted. The spin-forbidden excitations are calculated to be too large, but the ab initio method agrees with experiment in identifying the trans difluoro compound as a 2T_1 emitter and the other substituted complexes as 2E emitters. Moreover, at the ab initio level, insight is gained into the origin of the splitting of the 2E_g parentage in tetragonal chromium(III) complexes.

I. Introduction

The ligand field spectra and the photochemical substitution reactions of chromium(III) ammine compounds have led to a huge amount of experimental data, which have been collected in a large number of reviews and monographs.^{1–11}

To a great extent, the experimental work has been stimulated by ligand field theory. The ligand field model has been very useful for the assignment of experimental band positions,^{12–16} and it forms the basis for a successful rationalization of the observed photochemistry.^{17–20}

It is surprising that chromium(III) ammine compounds have received so little attention from other theoretical lines of approach. Apart from a set of extended Hückel calculations carried out by Zink,²¹ no molecular orbital studies appear to have been published thus far. Still, the importance of such studies can hardly be questioned. For one thing, it is a generally accepted assumption of ligand field theory that the NH_3 ligand does not contribute to π bonding and $\pi_{\text{NH}_3} = 0$ is generally used as a reference equation; molecular orbital calculations can place this hypothesis in its proper perspective. It is also well-known that the NH_3 ligand is of intermediate ligand field strength. Therefore, it would be interesting to compare the molecular orbital results for $\text{Cr}(\text{NH}_3)_6^{3+}$ with those for CrF_6^{3-} , a weaker field complex, and those for $\text{Cr}(\text{CN})_6^{3-}$, a stronger field complex. Calculations for the latter two complexes have both been published before.^{22,23} Furthermore,

molecular orbital results on chromium(III) ammine compounds may be helpful in understanding the large 2E_g splitting for $\text{Cr}(\text{NH}_3)_5\text{X}^{2+}$ ($\text{X} = \text{Cl}^-, \text{Br}^-, \text{I}^-, \text{ONO}^-, \text{H}_2\text{O}, \text{NCO}^-$) complexes.^{24–30} Conventional ligand field calculations yield 2E_g splittings that are 1 order of magnitude smaller than the observed ones.^{29,30} Flint et al. suggested that this discrepancy arose because of the use of spherical electron repulsion parameters.²⁹ More recently, it has been shown that the 2E_g splitting can be considerably enlarged by mixing some ligand character in the d_{xz} and d_{yz} orbitals.²⁶ It was found that a ligand contribution of only 1.6% could reproduce the experimental 2E_g splittings of about 200 cm^{-1} . However, the importance of such a contribution has never been proven by means of rigorous molecular orbital calculations.

In this paper, the first ab initio molecular orbital study on a number of chromium(III) ammine complexes is presented. This study is carried out at the restricted Hartree–Fock ligand field CI level (RHF/LFCI), and the selected compounds are $\text{Cr}(\text{NH}_3)_6^{3+}$, the monosubstituted $\text{Cr}(\text{NH}_3)_5\text{F}^{2+}$ complex, two trans-disubstituted compounds, namely *trans*- $\text{Cr}(\text{NH}_3)_4\text{F}_2^+$ and *trans*- $\text{Cr}(\text{NH}_3)_4\text{Cl}_2^+$, and one cis-disubstituted complex, namely *cis*- $\text{Cr}(\text{NH}_3)_4\text{F}_2^+$. The study comprises a detailed analysis of these molecules at the orbital level and a calculation of the ligand field spectra. The ab initio results are discussed within the framework of a ligand field analysis of the different complexes and are compared with the available experimental data. In a number of subsequent papers, the photochemical substitution reactions of chromium(III) ammine compounds will be discussed.

II. Computational Details

For each complex, we calculated the weighted average of all ligand field states,³¹ which will be denoted as $\text{Av}(d^3)$, by means of the SYMOL program.³² This program is based on Roothaan's restricted Hartree–Fock formalism for open-shell systems.³³ The $\text{Av}(d^3)$ orbitals were used to carry out ligand field CI calculations considering all states originating from the d^3 configuration. For this purpose, a general computer program was developed that constructs all possible Slater determinants for an

- Balzani, V.; Carassiti, V. *Photochemistry of Coordination Compounds*; Academic Press: London, 1970.
- Kirk, A. D. *Mol. Photochem.* **1973**, *5*, 127.
- Adamson, A. W.; Fleischauer, P. D. *Concepts of Inorganic Photochemistry*; Wiley: New York, 1975.
- Wrighton, M. S. *Top. Curr. Chem.* **1976**, *65*, 37.
- Adamson, A. W. *Pure Appl. Chem.* **1979**, *51*, 313.
- Kirk, A. D. *Coord. Chem. Rev.* **1981**, *39*, 225.
- Vanquickenborne, L. G.; Ceulemans, A. *Coord. Chem. Rev.* **1983**, *48*, 157.
- Larkworthy, L. F. *Coord. Chem. Rev.* **1984**, *57*, 189.
- Endicott, J. F.; Ramasami, T.; Tamilarasan, R.; Lessard, R. B.; Ryu, C. K. *Coord. Chem. Rev.* **1987**, *77*, 1.
- Mønsted, L.; Mønsted, O. *Coord. Chem. Rev.* **1989**, *94*, 109.
- Forster, L. S. *Chem. Rev.* **1990**, *90*, 331.
- Perumareddi, J. R. *J. Phys. Chem.* **1967**, *71*, 3155.
- Perumareddi, J. R. *Coord. Chem. Rev.* **1969**, *4*, 73.
- Lowry, R. K.; Perumareddi, J. R. *J. Phys. Chem.* **1970**, *74*, 1371.
- Glerup, J.; Mønsted, O.; Schäffer, C. E. *Inorg. Chem.* **1976**, *15*, 1399.
- Schmidtke, H.-H.; Degen, J. *Struct. Bonding* **1989**, *71*, 99.
- Vanquickenborne, L. G.; Ceulemans, A. *J. Am. Chem. Soc.* **1977**, *99*, 2208.
- Vanquickenborne, L. G.; Ceulemans, A. *J. Am. Chem. Soc.* **1978**, *100*, 475.
- Vanquickenborne, L. G.; Ceulemans, A. *Inorg. Chem.* **1979**, *18*, 897.
- Vanquickenborne, L. G.; Ceulemans, A. *Inorg. Chem.* **1979**, *18*, 3475.
- Zink, J. I. *J. Am. Chem. Soc.* **1974**, *96*, 4464.
- Vanquickenborne, L. G.; Haspeslagh, L.; Hendrickx, M.; Verhulst, J. *Inorg. Chem.* **1984**, *23*, 1677.

- Pierloot, K.; Vanquickenborne, L. G. *J. Chem. Phys.* **1990**, *93*, 4155.
- Shepard, W. N.; Forster, L. S. *Theor. Chim. Acta (Berlin)* **1971**, *20*, 135.
- Decurtins, S.; Güdel, H. U.; Neuschwander, K. *Inorg. Chem.* **1977**, *16*, 796.
- Schmidtke, H. H.; Adamsky, H.; Schönherr, T. *Bull. Chem. Soc. Jpn.* **1988**, *6*, 59.
- Riesen, H. *Inorg. Chem.* **1988**, *27*, 4677.
- Lee, K. W.; Hoggard, P. E. *Inorg. Chem.* **1988**, *27*, 907.
- Flint, C. D.; Matthews, A. P. *J. Chem. Soc., Faraday Trans. 2* **1973**, *69*, 419.
- Schönherr, T.; Schmidtke, H. H. *Inorg. Chem.* **1979**, *18*, 2726.
- The frozen orbital results based on the $\text{Av}(d^3)$ orbitals are hardly different from the results that would be obtained by carrying out single Hartree–Fock calculations for each individual state. For instance, for the ground state of $\text{Cr}(\text{NH}_3)_6^{3+}$, the frozen orbital energy amounts to -1379.632060 hartrees; the SCF energy to -1379.634137 hartrees. The difference between these numbers is only 456 cm^{-1} . Still smaller deviations are expected for the excited states as they are close in energy to the $\text{Av}(d^3)$ level.
- Van der Velde, G. A. Ph.D. Thesis, Rijksuniversiteit Groningen, The Netherlands, 1974.
- Roothaan, C. C. J. *Rev. Mod. Phys.* **1951**, *23*, 69; **1960**, *32*, 179.

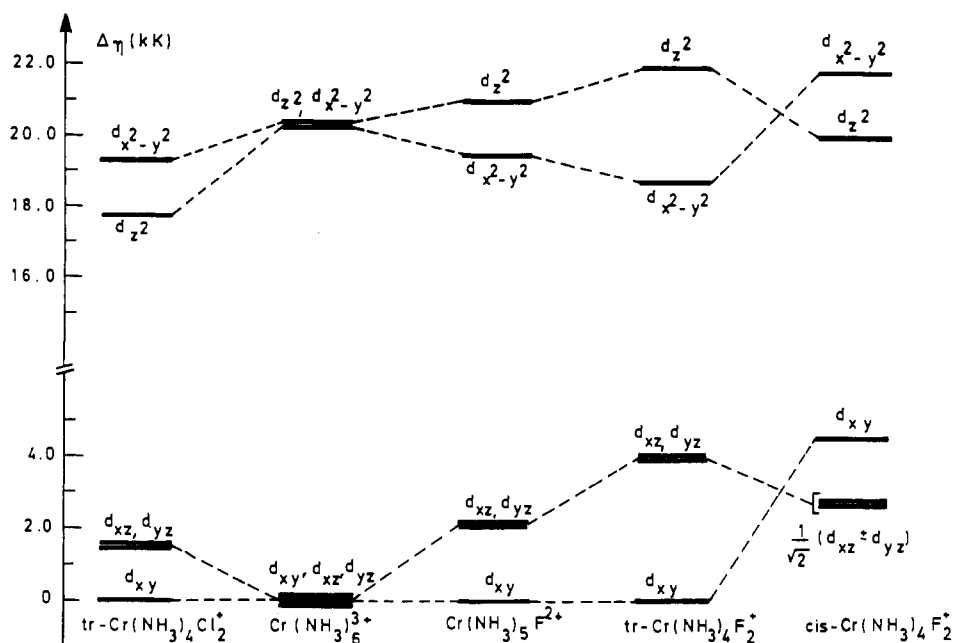


Figure 1. Ab initio $\text{Av}(\text{d}^3)$ \bar{d} orbital energy diagram (in 10^3 cm^{-1} ($=\text{kK}$)) for the five complexes under consideration. For $\text{Cr}(\text{NH}_3)_6^{3+}$, $\text{Cr}(\text{NH}_3)_5\text{F}_2^{2+}$, and the two trans-substituted complexes, the d_{xy} orbital is arbitrarily set at equal energy. For the cis compound, the zero of the energy scale was taken to be the same as for $\text{trans-Cr}(\text{NH}_3)_4\text{F}_2^+$.

arbitrary d^N system, sets up the relevant interaction matrix and carries out its diagonalization.³⁴

The basis sets we used were chosen so as to obtain near Hartree-Fock limit results and to guarantee a balanced description of the metal and the ligands. The Cr^{3+} ion was described by a (15s,11p,6d/11s,8p,4d) basis set, whose exponents and contraction scheme have been detailed previously.^{35,36} For F and N, we adopted the (9s,5p/5s,3p) bases proposed by Huzinaga and Dunning, and for the hydrogen atom, a (4s/3s) basis set.³⁷ The Cl atom was described by the (12s,9p/6s,5p) nonsegmented basis set that was introduced by Dunning.³⁸

The calculations were performed on idealized geometries, keeping all ligand-metal-ligand bond axes at 90° and using only one set of bond distances. The Cr-N bond length was taken to be 2.07 Å, the average value for a number of $\text{Cr}(\text{NH}_3)_6^{3+}$ ions in different crystal environments.³⁹⁻⁴⁴ For the $\text{Cr}(\text{NH}_3)_5\text{F}_2^{2+}$ complex, no experimental structure determinations are available. Therefore, the Cr-F distance was set equal to the average Cr-F bond length of $\text{trans-Cr}(\text{NH}_3)_4\text{F}_2^+$ and $\text{cis-Cr}(\text{NH}_3)_4\text{F}_2^+$, i.e. 1.89 Å.⁴⁵ The Cr-Cl distance was taken to be the experimental Cr-Cl bond length of the $\text{trans-Cr}(\text{NH}_3)_4\text{Cl}_2^+$ complex, namely 2.33 Å.⁴⁶ For the hydrogen atoms, no X-ray data were used. It is well-known that X-H (X = N, C, O) distances obtained by X-ray diffraction are much too low.⁴⁷ Therefore, the N-H bond length and the H-N-H angle were taken to be identical with those of the free NH_3 molecule: $R(\text{N-H}) = 1.02 \text{ \AA}$ and $\theta(\text{H-N-H}) = 106.6^\circ$.⁴⁷ Each Cr-NH₃ unit was assumed to have C_{3v} symmetry and a maximal symmetry arrangement was chosen for the ammonia ligands: C_{4v} for $\text{trans-Cr}(\text{NH}_3)_4\text{X}_2^+$, C_{2v} for $\text{Cr}(\text{NH}_3)_6^{3+}$ and $\text{cis-Cr}(\text{NH}_3)_4\text{F}_2^+$, and C_3 for $\text{Cr}(\text{NH}_3)_5\text{X}^{2+}$. For $\text{Cr}(\text{NH}_3)_5\text{F}_2^{2+}$ and the two trans complexes, the hetero-

Table I. Ligand Field Energy Expressions for the Energies of the Five \bar{d} Orbitals for $\text{Cr}(\text{NH}_3)_6^{3+}$, $\text{Cr}(\text{NH}_3)_5\text{X}^{2+}$, $\text{trans-Cr}(\text{NH}_3)_4\text{X}_2^+$, and $\text{cis-Cr}(\text{NH}_3)_4\text{X}_2^+$, Where N Stands for the NH_3 Ligand

orbital	$\text{Cr}(\text{NH}_3)_6^{3+}$	$\text{Cr}(\text{NH}_3)_5\text{X}^{2+}$	$\text{trans-Cr}(\text{NH}_3)_4\text{X}_2^+$	$\text{cis-Cr}(\text{NH}_3)_4\text{X}_2^+$
d_{xy}	$4\pi_N$	$4\pi_N$	$4\pi_N$	$2\pi_N + 2\pi_X$
d_{xz}	$4\pi_N$	$3\pi_N + \pi_X$	$3\pi_N + 2\pi_X$	$3\pi_N + \pi_X$
d_{yz}	$4\pi_N$	$3\pi_N + \pi_X$	$2\pi_N + 2\pi_X$	$3\pi_N + \pi_X$
d_{z^2}	$3\sigma_N$	$2\sigma_N + \sigma_X$	$\sigma_N + 2\sigma_X$	$3/2\sigma_N + 1/2\sigma_X$
$\text{d}_{x^2-y^2}$	$3\sigma_N$	$3\sigma_N$	$3\sigma_N$	$3/2\sigma_N + 3/2\sigma_X$

ligands are situated on the z axis; for $\text{cis-Cr}(\text{NH}_3)_4\text{F}_2^+$ one fluorine is situated on the x axis and the other on the y axis.

III. Results and Discussion

A. General Features of the $\text{Av}(\text{d}^3)$ Calculation. As has been noted for other transition-metal complexes,^{22,48,49} the $\text{Av}(\text{d}^3)$ orbitals for the five chromium(III) compounds under consideration fall into two categories: they are predominantly metal centered (metal character greater than 87%) or they are predominantly ligand centered (metal character smaller than 16%) with nothing in between. This subdivision follows from a Mulliken population analysis and finds additional support by a component analysis of the orbital energies. The orbitals with predominant metal character have a significantly greater interelectronic repulsion energy, a much larger kinetic energy and a much larger (negative) electron-nuclear attraction energy than the ligand-centered orbitals. As it has been pointed out before,²² to some extent this very clear-cut distinction supports one of the basic postulates of ligand field theory, where a complex is described as a perturbed metal ion and where the ligand orbitals are not explicitly considered.

1. Energies of the Dominant \bar{d} Orbitals. Figure 1 shows the orbital energy diagram of the $\text{Av}(\text{d}^3)$ molecular orbitals with predominant metal \bar{d} character, henceforth denoted as \bar{d} . In each complex, the open shell \bar{d}_o orbitals have a higher energy than any of the other $\text{Av}(\text{d}^3)$ MO's. The open shell \bar{d}_o orbitals however, are situated within the energetic range of the ligand σ orbitals. The same situation has been observed several times before,^{22,48,49} and it was shown that this energetic ordering hardly affects the ligand field description of transition-metal complexes. Indeed,

(34) FRORB was written by K. Pierloot, Laboratory of Quantum Chemistry, University of Leuven, Belgium.

(35) Vanquickenborne, L. G.; Verhulst, J. *J. Am. Chem. Soc.* **1983**, *105*, 1769.

(36) Vanquickenborne, L. G.; Verhulst, J.; Coussens, B.; Hendrickx, M.; Pierloot, K. *J. Mol. Struct. (THEOCHEM)* **1987**, *153*, 227.

(37) Dunning, T. H. *J. Chem. Phys.* **1970**, *53*, 2823. Huzinaga, S. *J. Chem. Phys.* **1965**, *42*, 1293.

(38) Veillard, A. *Theor. Chim. Acta* **1968**, *12*, 405. Dunning, T. H. *Chem. Phys. Lett.* **1970**, *7*, 423.

(39) Raymond, K. N.; Meek, D. W.; Ibers, J. A. *Inorg. Chem.* **1968**, *7*, 1111.

(40) Goldfield, S. A.; Raymond, K. N. *Inorg. Chem.* **1971**, *10*, 2604.

(41) Von Wiegardt, K.; Weiss, J. *Acta Crystallogr.* **1972**, *B28*, 529.

(42) Clegg, W.; Greenhalgh, D. A.; Straughan, B. P. *J. Chem. Soc., Dalton Trans.* **1975**, 2591.

(43) Clegg, W. *Acta Crystallogr.* **1976**, *B32*, 2907.

(44) Clegg, W. *J. Chem. Soc., Dalton Trans.* **1982**, 593.

(45) Brenčić, J. V.; Čeh, B.; Leban, I. *Monatsh. Chem.* **1981**, *112*, 1359.

(46) Brenčić, J. V.; Leban, I.; Zule, J. *Z. Anorg. Allg. Chem.* **1985**, *521*, 199.

(47) Hamilton, W. C.; Ibers, J. A. *Hydrogen Bonding in Solids*; Benjamin: New York, 1968.

(48) Vanquickenborne, L. G.; Hendrickx, M.; Hyla-Kryspin, I. *Inorg. Chem.* **1989**, *28*, 770.

(49) Vanquickenborne, L. G.; Hendrickx, M.; Hyla-Kryspin, I.; Haspelslagh, L. *Inorg. Chem.* **1986**, *25*, 885.

Table II. Percent Composition of the $Av(d^3)$ Orbitals with Predominantly Metal d Character for the Four Complexes under Consideration, Based on the Mulliken Gross Populations

complex	moiety	\bar{d}_π		\bar{d}_σ	
		\bar{d}_{xy}	$\bar{d}_{xz,yz}$	$\bar{d}_{x^2-y^2}$	\bar{d}_{z^2}
$Cr(NH_3)_6^{3+}$	Cr	99.2	99.2	86.9	86.9
	NH ₃	0.8	0.8	13.1	13.1
$Cr(NH_3)_5F^{2+}$	Cr	99.2	97.8	87.9	88.1
	NH ₃	0.8	0.6	12.1	7.5
	F		1.6		4.3
<i>cis</i> - $Cr(NH_3)_4F_2^+$	Cr	97.0	98.1	89.0	89.0
	NH ₃	0.4	0.4	4.8	9.0
	F	2.6	1.5	6.2	2.1
<i>trans</i> - $Cr(NH_3)_4F_2^+$	Cr	99.3	97.2	88.9	89.1
	NH ₃	0.7	0.4	11.1	3.7
	F		2.4		7.2
<i>trans</i> - $Cr(NH_3)_4Cl_2^+$	Cr	99.3	97.1	87.8	85.8
	NH ₃	0.7	0.4	12.2	3.9
	Cl		2.5		10.1

because orbital energy differences $\Delta\eta$ are not simply or directly related to state energy differences ΔE , it does not prevent the d - d transitions from having the lowest energy.²²

Within the "d-only" additive ligand field model, the energies of the d orbitals can be described by a single set of ligand field parameters. These energy expressions are listed in Table I and can be compared with the results of Figure 1.

According to the ligand field model, the d_{xz} and d_{yz} orbitals of the *cis* compound are degenerate. This degeneracy is a result of the effective holohedral D_{4h} symmetry of *cis*- $Cr(NH_3)_4F_2^+$. Obviously, the holohedral symmetry of the *cis* compound is very well realized by our *ab initio* calculations. As a matter of fact, the splitting of the \bar{d}_{xz} and \bar{d}_{yz} orbitals amounts to only 160 cm^{-1} . This small value reflects the nearly pure metal $3d$ character of the involved molecular orbitals.

Another prediction of ligand field theory is that the splitting of the t_{2g} and e_g orbitals in the monosubstituted complex is the same as for the *cis* compound (except for the sign) and half the splitting for *trans*- $Cr(NH_3)_4F_2^+$. Therefore, the ratio of the d orbital splittings is expected to be 1:2:(-1) for $Cr(NH_3)_5F^{2+}$, *trans*- $Cr(NH_3)_4F_2^+$, and *cis*- $Cr(NH_3)_4F_2^+$ respectively. Again, this prediction is confirmed rather nicely by our *ab initio* results. For the t_{2g} orbitals, the actual numbers are 2090, 3926, and -1792 cm^{-1} ; for the e_g shell they are calculated to be 1478, 3290, and -1765 cm^{-1} .

In ligand field theory it is also assumed that a substitution of the amines along the z axis has no effect on the $d_{xy} - d_{x^2-y^2}$ separation. According to our *ab initio* results however, such a substitution reduces that separation to some extent. Quantitatively, the variation of the $\bar{d}_{xy} - \bar{d}_{x^2-y^2}$ separation appears to be almost negligible: in the *trans*-difluoro compounds, the energy difference between the two orbitals is only $\sim 8\%$ smaller than in the parent octahedral compound.

The $\Delta\eta$ values of Figure 1 also have the same sign as in ligand field theory. Indeed, in $Cr(NH_3)_5F^{2+}$ and the two *trans* complexes, the d_{xz} and d_{yz} orbitals are more destabilized than the d_{xy} orbital. This indicates that $\pi_N - \pi_X$ ($X = F^-, Cl^-$) must be positive or, in other words, that the F^- and Cl^- ions are stronger π donors than the NH_3 molecule. Moreover, Figure 1 shows that the splitting of the t_{2g} orbitals is smaller in the *trans*-dichloro than in the *trans*-difluoro compound. Therefore, in agreement with the ligand field model, the *ab initio* $\Delta\eta$ values classify the Cl^- ligand as a weaker π donor than the F^- ion. As for the e_g shell, one can notice an energy splitting of different sign in the dichloro complex than in $Cr(NH_3)_5F^{2+}$ and the *trans* difluoro compound. These splittings reflect the fact that the Cl^- ion is a weaker σ donor than NH_3 while the F^- ligand is a stronger σ donor than the NH_3 molecule.⁵⁰

2. Composition and Repulsion Parameters of the \bar{d} Orbitals.

Table II shows the composition of the open-shell d orbitals. As can be seen, the \bar{d}_σ orbitals are significantly more covalent than the \bar{d}_π orbitals: for the $\bar{d}_{x^2-y^2}$ and \bar{d}_{z^2} orbitals, the ligand character is at least $\sim 11\%$; for the \bar{d}_π orbitals on the other hand, it is at most only $\sim 3\%$. This corresponds to the expected picture that the σ interactions are much stronger than the π interactions. In the monosubstituted $Cr(NH_3)_5F^{2+}$ complex and the two *trans* complexes, the composition of $\bar{d}_{x^2-y^2}$ and \bar{d}_{xy} reflects the bonding of the NH_3 ligand, while \bar{d}_{z^2} and $\bar{d}_{xz,yz}$ show the combined effect of NH_3 and the heteroligands. Interestingly, the ligand character of the \bar{d}_{xy} orbitals is almost zero. This supports the ligand field idea that the π -donation of NH_3 is negligible ($\pi_{NH_3} = 0$). Cl^- and F^- are obviously better π -donors.

According to the composition of the \bar{d}_{z^2} orbital in $Cr(NH_3)_6^{3+}$, $Cr(NH_3)_5F^{2+}$, *trans*- $Cr(NH_3)_4F_2^+$, and *trans*- $Cr(NH_3)_4Cl_2^+$, Cl^- should be classified as a better σ -donor and F^- as a poorer σ -donor than NH_3 . This is exactly the opposite sequence as the one resulting from a consideration of the $\Delta\eta$ values in section III.A.1. However, it is clear that there is not really a contradiction. The classification in the section III.A.1 is based on energetic considerations and should therefore correspond to the classification of the ligands in the spectrochemical series. And indeed, in the *spectrochemical series*, the different ligands are classified as follows:^{51,52}



The figures in Table II however represent the mixing of metal d and ligand orbitals and are thus indicative for the covalency of the different metal-ligand bonds. As such they should rather be compared to the *nephelauxetic series* of ligands. Indeed, a transfer of electronic charge from the ligands to the central metal ions causes an expansion of the metal d orbitals, thereby lowering the d - d repulsion energy. This phenomenon is known as the nephelauxetic effect.⁵¹⁻⁵³ The figures in Table II suggest that the $Cr-Cl$ bond is more covalent than the $Cr-F$ bond, which is in turn more covalent than the $Cr-NH_3$ bond. This does indeed correspond to the empirical *nephelauxetic series*, which classifies the different ligands as follows:^{51,52}



Alternatively, the covalency of a given complex can be measured at the *ab initio* level by means of the average (\bar{d}, \bar{d}) repulsion. This repulsion is given by

$$(\bar{d}, \bar{d}) = \frac{1}{45} [15(t_2, t_2) + 6(e, e) + 24(t_2, e)] \quad (3)$$

where (t_2, t_2) and (e, e) respectively stand for the average repulsion between two t_2 or two e electrons and (t_2, e) represents the average repulsion between one t_2 and one e electron. These quantities are given by the following expression:

$$(\lambda, \nu) = \frac{1}{M} \sum_{\rho=1}^{d_\lambda} \sum_{q=1}^{d_\nu} (2J_{\rho q} - K_{\rho q}) \quad (4)$$

Here, the summation runs over the space orbitals, λ and ν stand for the t_2 or e shell, d_λ and d_ν stand for the spatial degeneracies and M is proportional to the number of different two-electron interactions.

$$M = 2d_\lambda d_\nu \text{ when } \lambda \neq \nu$$

$$M = d_\nu(2d_\nu - 1) \text{ when } \lambda = \nu \quad (5)$$

For a given complex, the average (\bar{d}, \bar{d}) repulsion is smaller than that in the free ion. This reduction is caused by two effects postulated by Jørgensen.^{51,52} The term "central field" covalency

(50) Hartree-Fock calculations are known to yield the wrong orbital level order (as compared to the ligand field expressions) in other substituted complexes; a typical example is the cobalt(III) cyanide complexes.^{48,49} However, when the state energy level splittings are considered, the SCF calculations always agree with the semiempirical conclusions.

(51) Jørgensen, C. K. *Modern Aspects of Ligand Field Theory*; North-Holland Publishing Company: Amsterdam, 1971.

(52) Gerloch, M.; Slade, R. C. *Ligand-field Parameters*; Cambridge University Press: Cambridge, England, 1973.

(53) Gerloch, M. *Coord. Chem. Rev.* **1990**, *99*, 117.

Table III. Av(d^3) Average (d,d) Repulsion^a (in hartree) for the Free Chromium Ion and the Seven Complexes under Consideration and the Ratio of the Average (d,d) Repulsion of the Chromium Ion to (\bar{d},\bar{d}) of the Complex

complex	(d,d), (\bar{d},\bar{d})	[(d,d):Cr ³⁺]/[(\bar{d},\bar{d})]
Cr ³⁺	0.8176	1.0000
CrF ₆ ³⁻	0.7676	0.9388
<i>trans</i> -Cr(NH ₃) ₄ F ₂ ⁺	0.7485	0.9155
<i>cis</i> -Cr(NH ₃) ₄ F ₂ ⁺	0.7459	0.9123
Cr(NH ₃) ₅ F ²⁺	0.7431	0.9089
Cr(NH ₃) ₆ ³⁺	0.7405	0.9057
<i>trans</i> -Cr(NH ₃) ₄ Cl ₂ ⁺	0.7377	0.9023
Cr(CN) ₆ ³⁻	0.7105	0.8690

^a For the definition, see text (eq 3).

denotes the expansion of the metal d orbitals as a consequence of the donation of the ligands. The "symmetry restricted" covalency on the other hand, is the result of the formation of antibonding molecular orbitals by mixing some ligand character into the metal d orbitals. In Table III, the average (\bar{d},\bar{d}) repulsion energies for the five complexes under consideration are confronted with the free ion value. For comparison, we also included the CrF₆³⁻ and Cr(CN)₆³⁻ compounds in Table III. As can be seen, the ratio [(d,d):Cr³⁺]/[(\bar{d},\bar{d})] becomes larger as more NH₃ ligands are replaced by F⁻ ions: it varies from 0.9057 in Cr(NH₃)₆³⁺ to 0.9388 in CrF₆³⁻. On the other hand, replacing the NH₃ molecules by Cl⁻ or CN⁻ ligands leads to a decrease of the average (\bar{d},\bar{d}) repulsion energy. Therefore, it can be concluded that NH₃ is a more covalent ligand than F⁻ but a less covalent ligand than the Cl⁻ or CN⁻ ion. So, the variation of the ratio [(d,d):Cr³⁺]/[(\bar{d},\bar{d})] confirms the conclusions that were based on Table II and is perfectly in line with the empirical nephelauxetic series. However, in the next section we shall see that from a quantitative point of view the ab initio nephelauxetic reductions are definitely too small.

The composition of the $\bar{d}_{x^2-y^2}$ in the complexes Cr(NH₃)₆³⁺, Cr(NH₃)₅F²⁺, *trans*-Cr(NH₃)₄F₂⁺, and *trans*-Cr(NH₃)₄Cl₂⁺ in Table II reflects the changes of σ -donation of the equatorial ammine ligands with a varying degree of axial substitution. The amines are seen to donate somewhat less in the substituted compounds than in Cr(NH₃)₆³⁺. The effect is clearly larger for F⁻ than for Cl⁻. Moreover, it is proportional to the degree of substitution: the contribution of NH₃ in the $\bar{d}_{x^2-y^2}$ orbital decreases by 1% with each subsequent substitution of an axial NH₃ by F⁻.

The observed results in the ligand populations with a varying degree of substitution can be simply rationalized from a charge effect. Replacing an NH₃ ligand by an F⁻ or Cl⁻ ion brings more negative charge in the first coordination sphere, thereby slightly reducing the donation of the other ligands. Because the Cr-F distance is shorter than the Cr-Cl distance the F⁻ ions have a greater influence than the Cl⁻ ions. A similar effect has been noted upon progressive CN⁻ → OH⁻ substitution in cobalt(III) cyanide compounds.^{48,49} In the CN⁻ ion, the negative charge is distributed more or less equally over the carbon and the nitrogen atom. In OH⁻ however, the negative charge is entirely localized on the oxygen. As consequence, the CN⁻ ligands are better donors in Co(CN)₆³⁻ than in the mono substituted Co(CN)₅(OH)³⁻ compound, where in turn they behave as better donors than in the *trans*- and *cis*-Co(CN)₄(OH)₂³⁻ complexes.

3. Validity of the Angular Overlap Model. In a series of papers on the underlying structure of ligand field theory, Gerloch and Woolley^{54,55} have criticized two important aspects of the angular overlap model: (i) its MO oriented approach to the role of the d electrons and (ii) the postulate of parameter transferability. We will now briefly discuss both points from the perspective of our present ab initio results.

In the view of Gerloch and Woolley, the d orbitals are largely uninvolved in overlap with the ligand functions, and the primary bond formation occurs between the ligand orbitals and the 4s and

Table IV. Excitation Energies (cm⁻¹) for All Relevant Quartet-Quartet Transitions and for the Quartet-Doublet Transitions within the t_{2g}³ Configuration of Cr(NH₃)₆³⁺^a

transition ^b	LFT	ab initio ^c	expt
⁴ A ₂ → ² E	14 271	19 343, 19 346	15 267 ⁶⁰
→ ² T ₁	14 864	20 264, 20 284, 20 299	
→ ² T ₂	21 984	28 591, 28 631, 28 657	
→ ⁴ T ₂	21 540	19 565, 19 611, 19 625	21 552 ⁹
→ ⁴ T ₁	28 859	28 893, 28 900, 28 912	28 409 ⁹
→ ⁴ T ₁	46 261	45 077, 45 157, 45 261	

^a The ligand field and ab initio values are the result of a CI calculation considering all states originating from the d³ configuration. Within LFT, this CI calculation was carried out with the semi-empirical parameters of Table VI; the ab initio CI calculation was performed within a frozen orbital approach, using the Av(d^3) orbitals. ^b The parity subscript has been dropped. ^c The ab initio results show slight splittings of the degeneracies, due to the actual C_{2v} symmetry of the hexammine complex.

4p functions of the metal valence shell. This renders an overlap-based interpretation of AOM parameters meaningless. To some extent, this point is in agreement with our findings. As we have argued, the spectrochemical strength of the ligands does not correlate with overlap considerations. This does not mean though that the overlap between d orbitals and the ligand functions is entirely negligible. As an example, for the chromium(III) hexammine complex, we have found that the 3d σ metal character in the bonding 2p σ ligand combination of e_g symmetry amounts to 16%. This percentage is larger than the 4s and 4p contributions in the bonding combinations of a_{1g} (10%) and t_{1u} (2%) symmetry, respectively.

A second point, which Gerloch emphasizes, is the nontransferability of the AOM parameters.^{56,57} In his view, replacement of a ligand can give rise to extensive charge redistributions in the complex, thereby affecting the bonding properties of the other ligands. These redistributions are expected to be in accordance with Pauling's electroneutrality principle. As we have indicated, there are indeed small changes in donation with varying degree of substitution, confirming that a given metal-ligand bond in a transition-metal complex is not completely independent of the other bonds. Moreover, simple charge considerations allow one to rationalize the observed redistributions. However, for the complexes considered, the observed charge shifts are rather small and do not endanger the transferability of ligand field parameters. We will return to this point in more detail in the next section.

B. Ligand Field Spectra. 1. Experimental Data. For the chromium(III) ammine compounds considered here, several spectroscopic investigations are available.^{1-10,58-66} It appears that the transition energies are rather insensitive to the crystal environment. For instance, for [Cr(NH₃)₅F](ClO₄)₂ and [Cr(NH₃)₅F](NO₃)₂, the reported values differ by at most ~300 cm⁻¹.^{58,59}

For Cr(NH₃)₆³⁺ and the *trans*-dichloro compound, the absorption spectra show very little solvent dependence. The spectra of the fluoride-containing complexes however, exhibit much larger

- (56) Gerloch, M.; Woolley, R. G. *J. Chem. Soc., Dalton Trans.* **1981**, 1714.
 (57) Gerloch, M. In *Understanding Molecular Properties*; Avery, J. S., Dahl, J. P., Hansen, A., Eds.; Reidel: Dordrecht, The Netherlands, 1987; p 111.
 (58) Kyuno, E.; Kamada, M.; Tanaka, N. *Bull. Chem. Soc. Jpn.* **1967**, 1848.
 (59) Wright, R. E.; Adamson, A. W. *Inorg. Chem.* **1977**, *16*, 3360.
 (60) Zinato, E.; Lindholm, R.; Adamson, A. W. *J. Inorg. Nucl. Chem.* **1969**, *31*, 449.
 (61) Wirth, G.; Bifano, C.; Walters, R. T.; Linck, R. G. *Inorg. Chem.* **1973**, *12*, 1955.
 (62) Glover, S. G.; Kirk, A. D. *Inorg. Chim. Acta* **1982**, *64*, L137.
 (63) Glerup, J.; Schäffer, C. E. *Inorg. Chem.* **1976**, *15*, 1408.
 (64) Forster, L. S.; Rund, J. V.; Fucaloro, A. F. *J. Phys. Chem.* **1984**, *88*, 5012.
 (65) Forster, L. S.; Rund, J. V.; Fucaloro, A. F. *J. Phys. Chem.* **1984**, *88*, 5017.
 (66) Fucaloro, A. F.; Forster, L. S.; Glover, S. G.; Kirk, A. D. *Inorg. Chem.* **1985**, *24*, 4242.

(54) Gerloch, M.; Woolley, R. G. *Prog. Inorg. Chem.* **1984**, *31*, 371.

(55) Woolley, R. G. *Int. Rev. Phys. Chem.* **1987**, *6*, 93.

Table V. Excitation Energies (cm⁻¹) for All Relevant Quartet–Quartet Transitions and for the Quartet–Doublet Transitions within the t_{2g}³ Configuration of Cr(NH₃)₅F₂²⁺, *trans*-Cr(NH₃)₄F₂⁺, *trans*-Cr(NH₃)₄Cl₂⁺, and *cis*-Cr(NH₃)₄F₂⁺^a

transition ^b			Cr(NH ₃) ₅ F ₂ ²⁺			<i>trans</i> -Cr(NH ₃) ₄ F ₂ ⁺			<i>trans</i> -Cr(NH ₃) ₄ Cl ₂ ⁺			<i>cis</i> -Cr(NH ₃) ₄ F ₂ ⁺		
O _h	D _{4h}		LFT	ab initio ^c	expt	LFT	ab initio	expt	LFT	ab initio	expt	LFT	ab initio ^c	expt
⁴ A ₂ → ² E	⁴ B ₁ → ² A ₁	→ ² A ₁	14 275	19 220	15 152 ⁶⁰	14 276	19 325		14 192	18 912	14 500 ⁶⁰	14 183	18 999	15 175 ⁶⁰
		→ ² B ₁	14 209	19 122		14 132	19 011		14 196	19 016		14 247	19 130	
	→ ² T ₁	→ ² A ₂	14 859	20 129		14 852	20 202	14 225 ⁶⁰	14 831	19 881		14 813	20 085	
	→ ² T ₂	→ ² E	14 416	19 813, 19 813		13 314	18 931		14 372	19 785		14 408	19 727, 19 839	
		→ ² B ₂	21 933	28 344		21 869	28 402		21 594	27 571		21 598	27 625	
		→ ² E	22 209	28 429, 28 363		23 010	28 760		21 983	27 728		22 162	28 162, 28 175	
⁴ A ₂ → ⁴ T ₂	⁴ B ₁ → ⁴ B ₂	→ ⁴ B ₂	21 540	18 877	19 920 ⁵⁵	21 540	18 134	20 325 ⁵⁹	21 540	18 716	21 097 ⁵⁹	18 455	16 901	19 011 ⁵⁹
		→ ⁴ E	19 992	17 941, 17 964		18 434	16 561	18 692 ⁵⁹	17 102	15 742	16 920 ⁵⁹	19 993	17 307, 17 200	
	→ ⁴ T ₁	→ ⁴ A ₂	29 018	28 752	27 248 ⁵⁵	28 996	28 274	27 933 ⁵⁹	25 343	25 154	25 063 ⁵⁹	25 365	24 623	26 316 ⁵⁹
	→ ⁴ T ₁	→ ⁴ E	27 117	26 681, 26 698		25 385	24 918	24 691 ⁵⁹	26 277	25 714		27 587	26 802, 26 851	
		→ ⁴ A ₂	43 242	42 220		40 404	40 642	41 152 ⁵⁹	39 697	39 353		43 360	41 331	42 194 ⁵⁹
		→ ⁴ E	44 810	43 183, 43 084		43 361	41 641		41 401	40 305		41 781	40 456, 40 712	

^aThe ligand field and ab initio energies are the result of a CI calculation considering all states originating from the d³ configuration. Within LFT, this CI calculation was carried out with the semiempirical parameters of Table VI; the ab initio CI calculation was performed within a frozen orbital approach, using the Av(d³) orbitals. ^bThe parity subscript has been dropped. ^cWithin the actual symmetry which is C₃ for Cr(NH₃)₅F₂²⁺ and C_{2v} for the cis compound, the ab initio energies for the two components of each E state are slightly different.

solvent effects.^{62,63} On going from a hydroxylic solvent, such as water, to a non-hydroxylic solvent, such as DMF, the spectral band positions may shift by ~1000 cm⁻¹. Obviously, such spectral changes cannot be reproduced by ab initio calculations on the isolated complex ions.

In Tables IV and V, the experimental transition energies are taken from the most recent spectroscopic investigations. The spectral band positions of the spin-allowed quartet–quartet transitions were obtained from absorption measurements. They correspond to a single or double excitation from the π type t_{2g} shell to the σ type e_g shell. Two such transitions are observed in the spectrum of Cr(NH₃)₆³⁺ and the monosubstituted Cr(NH₃)₅F₂²⁺ compound. They have been assigned as ⁴A₂ → ⁴T₂ and ⁴A₂ → ⁴T₁(a), the more energetic ⁴A₂ → ⁴T₁(b) transition being masked by charge-transfer bands. In *trans*-Cr(NH₃)₄Cl₂⁺ the splitting of the ⁴A₂ → ⁴T₂ excitation can directly be observed. The absorption peak at 16 920 cm⁻¹ has been assigned as a ⁴B₁ → ⁴E transition and corresponds to an excitation from the (d_{xz}, d_{yz}) orbitals; the peak at 21 097 cm⁻¹ has been identified as the ⁴B₁ → ⁴B₂ transition, which corresponds to a d_{xy} → d_{x²-y²} excitation. In the spectra of the difluoro compounds, also the ⁴A₂ → ⁴T₁(b) transition shows up. No splitting of the quartet bands is observed in the spectrum of the cis complex, while for the trans compound not only the ⁴A₂ → ⁴T₂ excitation, but also the ⁴A₂ → ⁴T₁(a) transition gives rise to two separated absorption peaks. The maximum at 24 691 cm⁻¹ has been assigned as a ⁴B₁ → ⁴E(b) transition, corresponding to an excitation from the (d_{xz}, d_{yz}) orbitals; the absorption peak at 27 933 cm⁻¹ has been identified as a ⁴B₁ → ⁴A₂ transition, which is caused by the d_{xy} → d_z excitation.}

Very recently, Forster and co-workers made a detailed study of the emission spectra of chromium(III) ammine compounds in glassy solutions at 77 K.^{64–68} They found that all complexes emit from their lowest excited doublet state. However, depending on the octahedral percentage of the luminescent state, there appear to be two different classes of emitters. The so-called ²E emitters emit from levels that are derived from the octahedral ²E parentage; ²T₁ emitters emit from doublet components of octahedral ²T₁ origin. These two classes of emitters produce different emission spectra, have different nonradiative relaxation rates, and exhibit different solvent effects. For the ²E emitters, it has been found that the emission spectra are sharp, that the nonradiative relaxation rates are confined to a narrow range, (0.9–3.5) × 10⁻⁴ s⁻¹, and that the emitting states are only slightly affected by the solvent. On the other hand, ²T₁ emitters are characterized by broad spectra usually shifted to longer wavelengths in hydroxylic solvents. For the chromium(III) ammine compounds that form the subject of this paper, it has been found that *trans*-Cr(NH₃)₄F₂⁺ is a ²T₁ emitter, while the other complexes belong to the class of ²E em-

Table VI. Comparison of the Semiempirical Ligand Field Parameters with the Theoretical Ligand Field Parameters for Cr(NH₃)₆³⁺ [hexa], Cr(NH₃)₅F₂²⁺ [monoF], *trans*-Cr(NH₃)₄F₂⁺ [transF₂], *trans*-Cr(NH₃)₄Cl₂⁺ [transCl₂], and *cis*-Cr(NH₃)₄F₂⁺ [cisF₂] (cm⁻¹)^a

parameter	LFT	hexa	monoF	transF ₂	transCl ₂	cisF ₂
B	700	1022	1024	1027	1027	1028
C	3000	4013	3978	3999	3890	3942
σ _N	7180	6533	6292	6045	6289	5891
σ _F	7630		7859	7788		7788
σ _{Cl}	5560				5120	
π _F	1880		2074	1966		1809
π _{Cl}	900				732	
10Dq _N	21540	19599	18876	18135	18867	17673
10Dq _F	15370		15281	15500		16128
10Dq _{Cl}	13080				12432	

^aThe semiempirical parameters are taken from ref 7. For each complex, the theoretical parameters are obtained by a fitting of the ligand field CI energy expressions to the ab initio transition energies of Tables IV and V. They reproduce the ab initio values within 180 cm⁻¹. N stands for the NH₃ ligand.

itters. The reported emission wavenumbers are listed in Tables IV and V.

2. Ligand Field Spectra and the Additivity and Transferability Idea. Semiempirical ligand field calculations, based on transferability of metal–ligand interactions, are capable of rationalizing the experimental data, as described in section III.B.1. Tables IV and V display under the heading LFT the results of complete ligand field CI calculations within the d³ manifold, using the classical ligand field parameters, which are listed in Table VI. It can be seen that these results are at most ~2000 cm⁻¹ in error.

For the interconfigurational quartet–quartet transitions, a similar agreement between theory and experiment is found at the ab initio level.³¹ On the other hand, for the intraconfigurational quartet–doublet excitations, the ab initio results are systematically too large.^{22,69} Very recently, it has been shown that a satisfactory reproduction of the spin-forbidden band maxima at the ab initio level requires an extensive correlation treatment where both the Cr 3d, the Cr 3s, and the Cr 3p orbitals are included.²³ Clearly, such a correlation treatment is not necessarily required for the spin-allowed transitions.

A recent Hartree–Fock study of the progressive CN⁻ → OH⁻ substitution in Co(CN)₆³⁻ revealed that the ab initio excitation energies confirmed the classical field ideas quite nicely.^{48,49} It is interesting to see whether such a confirmation can also be found from the analysis of the ab initio spectra of the here considered chromium(III) compounds. For the sake of convenience, the calculated levels are visualized in Figure 2. Moreover, for each

(67) Fucaloro, A. F.; Forster, L. S. *Inorg. Chim. Acta* **1987**, *132*, 253.
 (68) Forster, L. S.; Mønsted, O. *J. Phys. Chem.* **1986**, *90*, 5131.

(69) Wachtors, A. J. H.; Nieuwpoort, W. C. *Phys. Rev. B: Solid State* **1972**, *5*, 291.

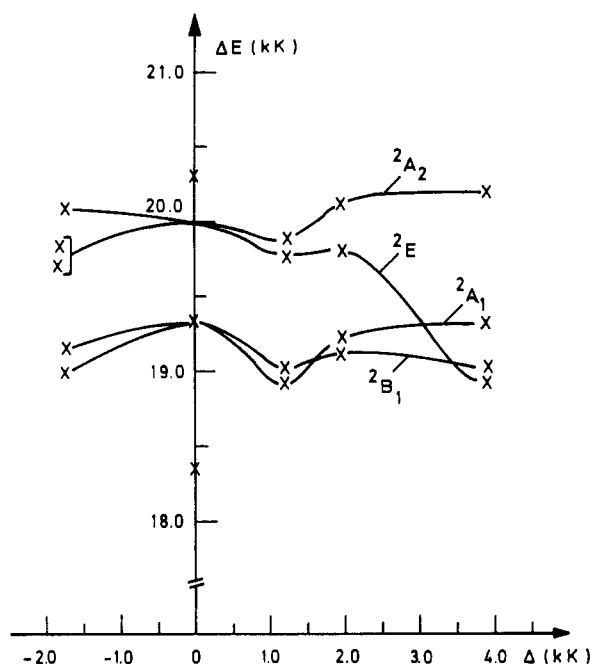
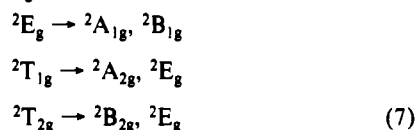


Figure 3. Ab initio energies of the lowest lying t_{2g}^3 doublets (see Tables V and VI) as a function of Δ defined in eq 9. The center of the figure ($\Delta = 0$) represents the parent octahedral states: 2E_g and ${}^2T_{1g}$. The other symmetry labels refer to the D_{4h} representation. The parity subscript has been dropped everywhere.

$\text{Cr}(\text{NH}_3)_6^{3+}$ is thus a 2E emitter. When the symmetry is lowered to D_{4h} , the octahedral t_{2g}^3 states are split as follows:



As has been shown in ref 71, the resulting energy splittings are entirely determined by the configuration interaction between the two equisymmetric tetragonal 2E_g states.

Using the appropriate $O_h \rightarrow D_{4h}$ subduction relations,⁷² it is easy to show that the zeroth-order ${}^2E_g(D_{4h})$ wave functions are approximately given by

$$\begin{aligned} {}^2T_{1g}: \quad |{}^2E_g x\rangle &= 1/\sqrt{2}[|yz\ xz\ \bar{x}z\rangle - |yz\ xy\ \bar{x}y\rangle] \\ |{}^2E_g y\rangle &= 1/\sqrt{2}[|xz\ xy\ \bar{x}y\rangle - |yz\ \bar{y}z\ xz\rangle] \\ {}^2T_{2g}: \quad |{}^2E_g x\rangle &= 1/\sqrt{2}[|yz\ xy\ \bar{x}y\rangle + |yz\ xz\ \bar{x}z\rangle] \\ |{}^2E_g y\rangle &= 1/\sqrt{2}[|xz\ xy\ \bar{x}y\rangle + |yz\ \bar{y}z\ xz\rangle] \end{aligned} \quad (8)$$

The interaction element between these 2E_g states is given by

$$\langle {}^2E_g({}^2T_{1g}) | H | {}^2E_g({}^2T_{2g}) \rangle = \frac{1}{2}[E[{}^2E_g(e_g^3)] - E[{}^2E_g(b_{2g}^2 e_g^1)]] \equiv \Delta \quad (9)$$

where $E[{}^2E_g(e_g^3)]$ and $E[{}^2E_g(b_{2g}^2 e_g^1)]$ represent the energies of the ${}^2E_g(e_g^3)$ and the ${}^2E_g(b_{2g}^2 e_g^1)$ states, which are described by

$$\begin{aligned} {}^2E_g(e_g^3): \quad |x\rangle &= |yz\ xz\ \bar{x}z\rangle \\ |y\rangle &= |yz\ \bar{y}z\ xz\rangle \\ {}^2E_g(b_{2g}^2 e_g^1): \quad |x\rangle &= |yz\ xy\ \bar{x}y\rangle \\ |y\rangle &= |xz\ xy\ \bar{x}y\rangle \end{aligned} \quad (10)$$

The ab initio energies of the lowest lying doublets as a function of Δ is depicted in Figure 3. As can be seen, at low tetragonal fields (low Δ values), the ${}^2A_{1g}$ and ${}^2B_{1g}$ components of the ${}^2E_g(O_h)$ parentage are below the ${}^2T_{1g}$ levels and the corresponding complex is a 2E emitter; at larger tetragonal fields, however, luminescence switches over to the ${}^2T_{1g}$ parentage as the degenerate ${}^2E_g(D_{4h})$

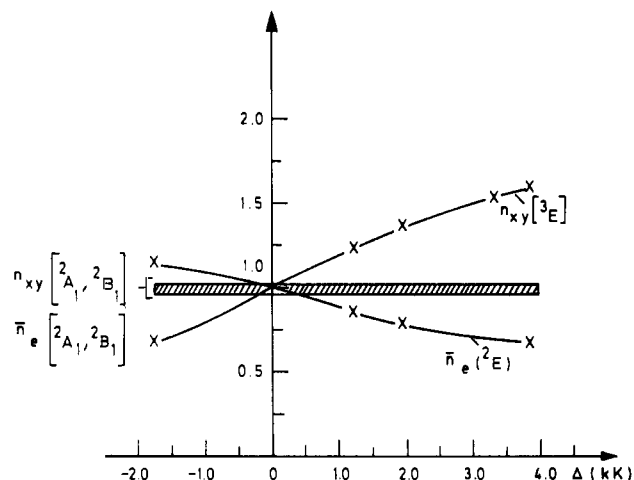


Figure 4. Orbital occupation numbers for the lowest lying t_{2g}^3 doublets as a function of Δ defined in eq 9. n_{xy} represents the population of the d_{xy} orbital; \bar{n}_e stands for the average occupation number of the d_{xz} and d_{yz} orbitals of e_g symmetry. In the ${}^2A_{1g}$ and ${}^2B_{1g}$ component of 2E_g origin, all occupation numbers are only slightly different from 1.0. This is indicated by the hatched area. The full lines represent the parity variation of the occupation numbers in the $D_{4h}({}^2E_g)$ state. The parity subscript has been dropped everywhere.

component of ${}^2T_{1g}$ origin drops below the ${}^2A_{1g}$ and ${}^2B_{1g}$ states.

The same conclusion was reached at the ligand field level.⁷¹ Here Δ simply amounts to twice the difference between the axial and equatorial π interactions

$$\Delta = \eta(xz, yz) - \eta(xy) = 2(\bar{\pi}_{ax} - \bar{\pi}_{eq}) \quad (11)$$

where for example $\eta(xy)$ represents the orbital energy of the d_{xy} orbital and $\bar{\pi}_{ax}$ stands for the average perturbation of the ligands on the $+z$ axis and the $-z$ axis. The cross-over point between 2E and ${}^2T_{1g}$ emission was found at $\Delta \sim 2000\text{ cm}^{-1}$. As can be seen from Figure 3, at the ab initio level, this transition point appears at larger tetragonal fields.

Composition of the Doublet States and Emission Behavior. The composition of the CI wave functions corresponding to the ${}^3E_g(O_h)$ and the ${}^2T_{1g}(O_h)$ states can be described by the orbital occupation numbers of the d orbitals. Due to the fact that all complexes under consideration have an effective symmetry which is very close to D_{4h} , the nondiagonal elements of the one-electron density matrix are negligibly small. Therefore, the occupation number of a particular molecular orbital corresponds to the sum of the orbital occupation numbers in the single-determinantal terms, weighted by the squares of the associated expansion coefficients. For instance, for the 2E_g components described in eq 8, the orbital occupation number of the d_{yz} orbital is exactly 1.0.

Figure 4 shows the ab initio orbital occupation numbers of the d orbitals in the 2E_g and ${}^2T_{1g}$ components of all complexes under consideration as a function of Δ (eq 9). For the ${}^2E_g({}^2T_{1g})$ state, these numbers correspond to the average occupation number of the d_{xz} and the d_{yz} orbital:

$$\bar{n}_e = \frac{1}{2}(n_{xz} + n_{yz}) \quad (12)$$

As can be seen, in $\text{Cr}(\text{NH}_3)_6^{3+}$ ($\Delta = 0$), all components have approximately one electron per t_{2g} orbital. In the substituted complexes, the same situation is observed for the ${}^2A_{1g}$ and the ${}^2B_{1g}$ states. On the other hand, for the 2E_g state of ${}^2T_{1g}$ origin, the d_{xy} orbital clearly has a different occupation than the d_{xz} and d_{yz} orbitals. As it appears, a positive Δ value causes a charge flow from d_{xz} and d_{yz} into the d_{xy} orbital while a negative Δ value results in the opposite shift of electron density. Hence, for either sign of Δ , the lower t_{2g} orbital always shows a population increase while the higher ones become more vacant.

Again, the above conclusions confirm the ligand field analysis of the emitting doublet levels which was performed on the first-order wave functions.⁷¹ Apparently, these functions have almost the same composition as our ab initio functions, the latter

(72) Griffith, J. S. *The Theory of Transition-Metal Ions*; Cambridge University Press: Cambridge, England, 1971.

being the result of a complete ligand field CI.

As it has already been pointed out by the authors of the ligand field study, the charge redistribution in the excited state of a 2T_1 emitter may induce solvational changes. In those interligand regions where the charge density decreases, the metal ion becomes more exposed to the environment, and as a consequence, solvent interactions may be enhanced. The opposite situation occurs where electron density is accumulated. In part, these solvational changes may be responsible for the broad emission spectra of 2T_1 emitters.

Furthermore, the charge redistribution in the 2E_g state changes the metal ligand bond strengths with respect to the ground state. At the ligand field level, these changes can be evaluated by means of the so-called bond indices,¹⁷ being a measure of the M-L bond energies.

When Δ is positive, the axial bonds have a larger bond index as compared to their ground-state value while the equatorial bonds have a smaller bond index. The opposite holds when Δ is negative.

Similar conclusions are obtained at the ab initio level. Here, a change in the bond strength of a particular M-L bond finds expression in a change in the ligand to metal donation which may be inferred from the results of a Mulliken population analysis or from density difference plots. As an example, Figure 5 shows the electron density shifts upon the ${}^4B_1 \rightarrow {}^2E$ excitation in the xy (Figure 5a) and in the yz (Figure 5b) planes of the *trans*-difluoro compound. One clearly observes the population of the d_{xy} zone and the depopulation of the d_{yz} orbital. Furthermore, one sees a strengthening of the Cr-F⁻ interactions as evidenced by the increased π donation of the F⁻ ions. On the other hand, the Cr-NH₃ interactions are hardly affected by the excitation process. Apparently, in the 2E state as well as in the ground state (see Table II), the Cr-NH₃ π interactions are negligible.

The increase in the Cr-F bond strengths can lead to sizable changes in bond lengths.⁷³ These changes may result in Franck-Condon progressions and appreciable Stokes shifts in accordance with the reported emission behavior of 2T_1 emitters.

Obviously, none of the above effects are expected for 2E emitters. As the t_{2g} orbitals of the 2E_g components have almost the same occupation number as in the ground state, solvational changes will be negligible. Moreover, the equilibrium geometry of the ${}^2A_{1g}$ and the ${}^2B_{1g}$ states will coincide with the ground-state equilibrium geometry. Hence, for 2E emitters, we expect a sharp-line luminescence spectrum, which is again in line with experiment.

4. Splitting of the 2E_g State. For several $\text{Cr}(\text{NH}_3)_5\text{X}^{2+}$ complexes the splitting of the octahedral 2E_g could be determined. Although it has been an object of controversy for a long time,²⁴⁻³⁰ it has been established very recently that the 2E_g splitting is rather large.²⁷ For instance, a detailed analysis of the crystalline powder absorption spectra for several $[\text{Cr}(\text{NH}_3)_5\text{Cl}]Y_2$ complexes, yielded 2E_g splittings of 169–192 cm^{-1} .²⁶ For each compound, the least energetic 2E_g component was identified as the 2A_1 state. Due to the large band superpositions and the lack of sufficient peak resolution, a similar analysis for $\text{Cr}(\text{NH}_3)_5\text{F}^{2+}$ was impossible. Also, for disubstituted chromium(III) ammine compounds, no experimental information on the 2E_g splitting is known. Therefore, our results must be considered as tentative predictions in this respect.

At the ligand field level, the large 2E_g splittings of the $\text{Cr}(\text{NH}_3)_5\text{X}^{2+}$ compounds pose a problem. For any reasonable choice of parameters, conventional AOM calculations appear to be incapable of generating splittings larger than 50 cm^{-1} .^{29,30} Recently, Schmidtke and co-workers²⁶ showed that the 2E_g splittings could be considerably enlarged by the introduction of the Stevens delocalization coefficients, i.e., by allowing a different LCAO expansion for the $b_2(d_{xy})$ orbital and the degenerate set of $e(d_{xz}, d_{yz})$ orbitals:

$$\psi(b_2) = \tau_{b_2}\varphi_M(b_2) + \lambda_{b_2}\varphi_L(b_2) \quad (13)$$

$$\psi(e) = \tau_e\varphi_M(e) + \lambda_e\varphi_L(e) \quad (14)$$

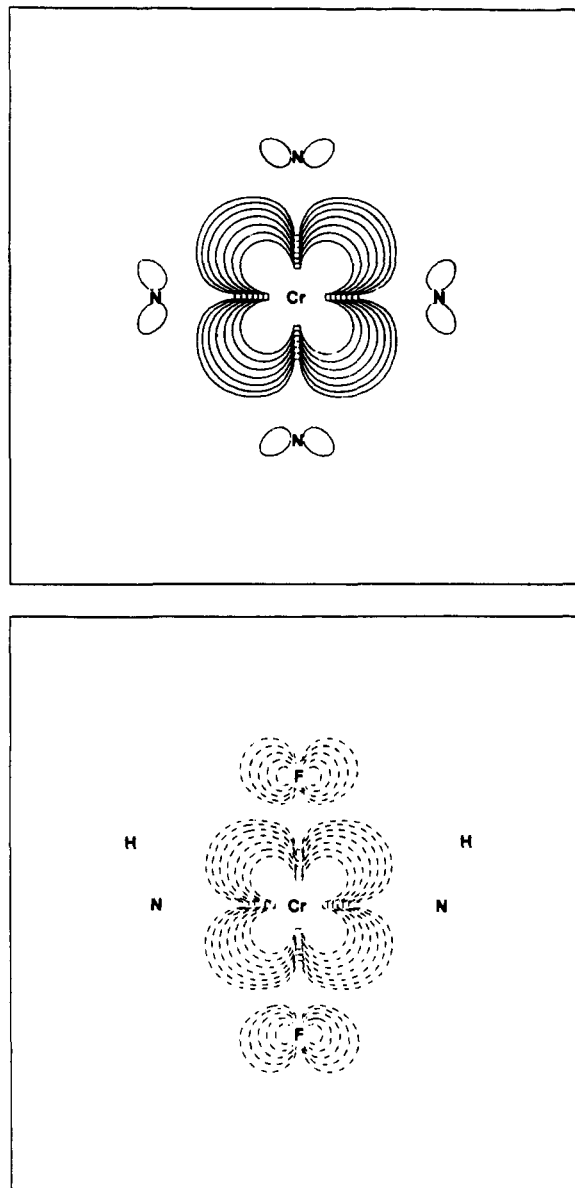


Figure 5. Total density difference plot $\rho({}^2E) - \rho({}^4B_1)$ for the *trans*- $\text{Cr}(\text{NH}_3)_4\text{F}_2^+$ complex. Part a (top) describes the density shifts in the xy plane on going from the 4B_1 to the 2E state of 2T_1 origin. Part b (bottom) describes the density shifts in the yz plane. Full contours correspond to an increase in electron density and dashed contours to a decrease in electron density. At the dotted lines $\Delta\rho = 0$. The values of the $\Delta\rho$ contours are ± 0.00025 , ± 0.0005 , ± 0.001 , ± 0.002 , ± 0.004 , ± 0.008 , and $\pm 0.016 \text{ au}^{-3}$.

Here, $\psi(i)$ denotes the molecular orbital of symmetry i , $\varphi_M(i)$ the metal d orbital of symmetry i , and $\varphi_L(i)$ the relevant linear combination of ligand orbitals of symmetry i . τ_i and λ_i are the corresponding LCAO expansion coefficients. Since the ligand field model assumes that $\pi_{\text{NH}_3} = 0$, the τ coefficient of b_2 symmetry was taken to be 1.0. For τ_e values only slightly smaller than 1, substantial 2E_g spacing could be obtained; e.g., for $\tau_e = 0.992$, one finds a spacing of 200 cm^{-1} .

As Schmidtke et al. demonstrated, the increase of the 2E_g splitting for $\tau_e < 1$, can be estimated from the first-order energy difference between the 2A_1 and the 2B_1 states. If the same set of orbitals is used for both states, this difference is given by

$$E({}^2B_1) - E({}^2A_1) = 2(K_{b_2e} - K_{ee}) \quad (15)$$

and as a function of τ_e and the Racah parameters B and C , one has

$$E({}^2B_1) - E({}^2A_1) = 2\tau_e^2(1 - \tau_e^2)(3B + C) \quad (16)$$

For $\tau_e < 1$, the above expression is positive.

Table VII. Ab Initio τ Coefficients, Exchange Integrals (in hartree) and Energy Differences between the 2A_1 and 2B_1 Components of 2E_g Origin (in cm^{-1}) for the *trans*-Cr(NH₃)₄Cl₂⁺ and the *trans*-Cr(NH₃)₄F₂⁺ complexes^a

	<i>trans</i> -Cr(NH ₃) ₄ Cl ₂ ⁺	<i>trans</i> -Cr(NH ₃) ₄ F ₂ ⁺
τ_{b_2}	0.996	0.996
τ_e	0.985	0.986
K_{b_2e}	0.031 919	0.032 231
K_{ee}	0.031 614	0.032 235
$E({}^2B_1) - E({}^2A_1)$	134	-2

^a The τ coefficients are defined in eqs 13 and 14; $E({}^2B_1) - E({}^2A_1)$ is given in eq 16. The b_2 orbital is of dominant d_{xy} character; the orbitals of e symmetry are of dominant d_{xz} and d_{yz} characters.

At the ab initio level, the τ coefficients and the relevant K integrals can be evaluated explicitly. The results for the two *trans* complexes are shown in Table VII. In agreement with the ligand field model, the ab initio method identifies the lowest 2E_g component of the *trans* dichloro compound as the 2A_1 state. Moreover, Table VII shows that the e orbitals are indeed more covalent than the b_2 orbital. More specifically, for the τ coefficients we have $\tau_e = 0.985 < \tau_{b_2} = 0.996$ and for the K integrals $K_{b_2e} = 0.0319$ hartree $> K_{ee} = 0.0316$ hartree. A somewhat different situation appears from the *trans*-difluoro compound. Although the τ coefficients are virtually identical with those of the *trans*-dichloro complex, the two K integrals are hardly different in this case. As a consequence, in the absence of CI effects, the 2A_1 state is calculated to have almost the same energy as the 2B_1 component. Clearly, the relative magnitude of the K integrals does not only depend on the τ coefficients, and the size of the mixing ligand orbitals is certainly an additional element that has to be taken into account. Indeed, the F orbitals are more compact than the Cl or the NH₃ orbitals; moreover, the CrF bond length is shorter than the CrN or CrCl bonds. As a consequence of these two factors, decreasing τ will have a smaller effect on the K integrals for F ligands than for Cl or NH₃ ligands. In the rationalization of Schmidtke et al., both factors were neglected.

When CI is taken into account, the 2E_g splittings of Table V are obtained. Apparently, CI causes a greater stabilization for the 2B_1 than for the 2A_1 component: for the *trans*-dichloro compound, the 2E_g splitting becomes smaller ($134 \text{ cm}^{-1} \rightarrow 104 \text{ cm}^{-1}$), for the *trans*-difluoro complex, CI leads to a larger 2A_1 - 2B_1 separation ($-2 \text{ cm}^{-1} \rightarrow -314 \text{ cm}^{-1}$). Although the LFT splittings

are systematically too small, it is worth mentioning that they always have the same sign as the ab initio splittings: for the *trans*-dichloro complex and the *cis* compound, the resulting $E({}^2B_1) - E({}^2A_1)$ (Table V) is positive; for Cr(NH₃)₅F₂⁺ and the *trans*-difluoro compound, this energy difference is negative.

IV. Conclusions

A Mulliken population analysis of the $Av(d^3)$ orbitals confirms the ligand field assumption that $\pi_{\text{NH}_3} = 0$. Yet, such an analysis does not support the idea that each metal ligand bond is a completely independent entity: it reveals that the donation of a particular ligand is influenced to some extent by the other ligands in the complex. However, it appears that these donation differences hardly affect the additivity and transferability postulate at the state level: the ab initio spectra for all complexes under consideration can be described quite reasonably with only one set of ligand field parameters. These parameters agree with the semiempirical values in classifying the Cl⁻ ion as the weakest σ donor, the weakest ligand field, and a weaker π donor than F⁻; F⁻ is identified as the strongest σ donor, having a smaller spectrochemical strength than the NH₃ molecule. These conclusions also follow from the relative order of the orbital energies in the $Av(d^3)$ state.

From a quantitative point of view, the quartet–quartet transition energies agree reasonably well with experiment. On the other hand, the quartet–doublet excitation energies are calculated much too large at the ab initio ligand field CI level. A better description of the spin-forbidden transitions requires an extensive treatment of electron correlation. It is gratifying though that already at the ligand field CI level, the ab initio results are in agreement with experiment in identifying the *trans*-difluoro compound as a 2T_1 emitter and the other substituted complexes as 2E emitters. Moreover, these results lead to a deeper understanding of the origin of the 2E_g splitting in tetragonal chromium(III) compounds. Apparently, this splitting does depend not only on the delocalization coefficients but also on the metal ligand bond lengths and the shape of the interacting ligand orbitals. Also, it is strongly affected by a complete ligand field CI within the d^3 manifold.

The nephelauxetic reduction in the different complexes has been analyzed by means of the average (d,d) repulsion. This led to the conclusion that NH₃ is a more covalent ligand than F⁻ but a less covalent ligand than the Cl⁻ or CN⁻ ions. This conclusion is perfectly in line with the nephelauxetic series.

Contribution from the School of Chemistry,
Queen's University of Belfast, Belfast BT9 5AG, Northern Ireland

Time-Resolved Resonance Raman Spectroscopy of [Cu(dmp)₂]⁺ in Solution

Keith C. Gordon and John J. McGarvey*

Received July 10, 1990

Pulsed and CW-laser-excited resonance Raman (RR) spectra are reported at a number of excitation wavelengths for the ground state and lowest energy metal-to-ligand charge-transfer (MLCT) excited state of [Cu(dmp)₂]⁺ (1) (dmp = bis(2,9-dimethyl-1,10-phenanthroline)). From analysis of the ground-state RR spectra, evidence has been obtained that three distinct transitions contribute to the MLCT absorption profile over the wavelength range 340–550 nm. The conclusions are in agreement with a recent independent analysis of the low-temperature UV–visible absorption spectrum of 1. The time-resolved RR spectra which are reported provide convincing evidence that the lowest MLCT excited state is localized, [(L)Cu^{II}(L⁻)]⁺, corroborating earlier, less extensive RR spectral data. The consequence of this assignment, that the effective symmetry of the thermally equilibrated MLCT excited state is C_{2v} or possibly C_2 , is considered in relation to a recent spectroscopic analysis of the MLCT excited states of related Cu(I) complexes.

Introduction

In recent papers, we have reported^{1,2} the resonance Raman spectra of the ground states and metal–ligand charge-transfer

(MLCT) excited states of copper(I) complexes with 2,9-disubstituted 1,10-phenanthroline ligands. The evidence supported a localized formulation, (L)Cu^{II}(L⁻) for the MLCT states. In the case where L = 2,9-diphenyl-1,10-phenanthroline (dpp), bands attributable to both neutral ligand L and radical anion L⁻ were observed, but for the 2,9-dimethyl-substituted analogue (dmp) at the probe wavelength (532 nm) used in the two color experiments carried out, depletion of the ground-state bands was ob-

(1) McGarvey, J. J.; Bell, S. E. J.; Bechara, J. N. *Inorg. Chem.* **1986**, *25*, 4325–4327.

(2) McGarvey, J. J.; Bell, S. E. J.; Gordon, K. C. *Inorg. Chem.* **1988**, *27*, 4003–4006.